Differences in Oxides on Large- and Small-Grained 304 Stainless Steel

D. R. BAER AND M. D. MERZ

The oxides formed on large-grained (~40 μm) and small-grained (~4 μm) 304 stainless steel oxidized in air at 800 °C have been examined and compared by Auger electron spectroscopy to learn more about the role of grain boundaries in the oxidation of the materials. For vacuum preannealed specimens, relatively thick iron oxides formed over the grains and thin, chromium-rich oxides formed over grain boudaries of large-grained material. The oxide formed over the entire surface of the small-grained material was a thin chromium-rich layer similar to that formed over grain boundaries of the large-grained samples. The oxidation of both small- and large-grained samples was consistent with selective formation of Cr_2O_3 at grain boundaries followed by a lateral diffusion of Cr and spreading of Cr_2O_3. A protective Cr_2O_3 layer formed readily on small-grained material but not on large-grained material. In contrast to the differences in oxide morphology for small- and large-grained preannealed specimens, oxide morphologies were similar for small- and large-grained material when the outer surface layer was removed by polishing after annealing and before oxidation tests. Surface differences, not adequately defined by Auger and SEM studies, caused marked changes in oxide morphologies for large-grained material. The difference in oxidation behavior before and after polishing was attributed to enhanced oxidation at grain boundaries during the vacuum preannealing treatment and to differences in defect concentrations in the surface region.

FORMATION of various oxides on alloy surfaces greatly depends on alloy composition, microstructure, and surface preparation. Fine-grained, sputter-deposited 304 stainless steel has been observed to be more resistant to oxidation than large-grained, wrought samples of the same material.[1] Although the exact role of grain boundaries in the oxidation of stainless steel is subject to some debate,[2] the improved resistance of the fine-grained, sputter-deposited material has been attributed to small grain size and the enhanced diffusion of chromium. We undertook this study to understand better the reason for the difference in composition and distribution of oxides formed on small- and large-grained stainless steel samples oxidized in air after being vacuum annealed. We were particularly interested in 1) the determination of the role of grain boundaries in the formation of the Cr-oxide regions on the fine-grained and coarse-grained materials and 2) comparison of these results with oxidation measurements in nickel-chromium alloys where grain-size effects on oxidation are also observed.[3-5]

The surface and near-surface distribution of elements in large- and small-grained samples is reported here. Auger electron spectroscopy (AES), in combination with sputter-depth profiling, was used to measure the elemental distribution on the outer surface of the samples and to determine elemental composition profiles of the oxides and alloys and their interface regions. The AES surface measurements were compared with earlier results obtained with an electron beam microprobe.[1] Because the surface composition of an alloy can influence the oxide that is formed,[6] AES was also used to examine the samples after vacuum-anneal pretreatment before oxidation. Specifically, we were interested in comparing the effects of the anneal on chromium and oxygen distributions in the coarse- and fine-grained materials.

Previous work[7,8] using AES to analyze surfaces of vacuum-annealed and oxidized stainless steel has not included study of the effects of grain size or grain boundaries on the oxides formed. Although Betz *et al*[8] recognized the desirability of observing the differences in composition between grains and grain boundaries, their equipment did not allow such observations. We have been able to directly observe grain-boundary composition on large-grained samples with fine-beam scanning Auger microscopy (SAM).

EXPERIMENTAL PROCEDURE

The surfaces of oxidized, large- (40 μm—ASTM grain size 6) and small-grained (4 μm— ASTM grain size 13) stainless steel samples were analyzed with a scanning Auger electron spectrometer.* Ion sputtering provided composition depth profiles. The sputtering rate was calibrated for Ta_2O_5 and the stated depths reported here refer to that standard; no corrections have been made for different sputtering rates of the different materials. The sputter depths indicated should, therefore, be considered as an approximate indication of depth into the material. It is known that differential sputtering of alloy components can also complicate interpretation of sputter-depth profiles by enhancing or depleting the apparent concentration of some elements. Although no blatant cases of this are apparent in the data, such effects could influence the semiquantitative results provided here. The elemental concentrations as deter-

* From Physical Electronics Industries.

D. R. BAER, Senior Scientist, Materials Department and M. D. MERZ, Technical Leader, Materials Department, both at Pacific Northwest Laboratory, Richland, WA 99352.

Manuscript submitted April 11, 1980.

ISSN 0360-2133/80/1211-1973$00.75/0

mined from the Auger data involve the use of empirical sensitivity factors[9] and are expected to be accurate within roughly 35 pct for each element. The data was reproducible to within 5 pct, however, and therefore, relative compositions can be compared even though the absolute elemental concentrations are accurate to only 35 pct.

Wrought (W) and sputter deposited (SD) samples were oxidized for 1/4, 30, and 120 h in air at 800 °C [Table I]. Some samples were annealed (A) but not oxidized in air. The sputter-deposited samples were from targets of the wrought commercial 304 stainless steel (Fe-18Cr-8Ni); details of the fabrication of samples by sputtering have been described elsewhere.[1] All samples were preannealed in quartz tubes that were evacuated to 10^{-6} torr and heated to 1000 °C for 2 h to stabilize grain size against additional grain growth during subsequent oxidation. The postanneal grain size of the wrought stainless steel was 40 μm and that of the sputter-deposited material was 3 to 4 μm. This treatment also produced lightly oxidized surfaces as was apparent in the subsequent Auger analysis. Most samples were then oxidized in air at 800 °C for the times indicated in Table I and cleaned sequentially in acetone, methanol and ethanol before insertion into the UHV chamber. A small number of samples were mechanically polished with 600 grit paper after the anneal and before oxidation. Because the samples were initially polished after fabrication, the samples polished between the anneal and oxidation are said to be repolished.

The scanning Auger electron beam had a minimum diameter of 2.5 μm, which determined the resolution of the system both for Auger analysis and for secondary electron images. Thus, for the large-grained samples, the spectrometer could be used in a mapping mode to indicate pictorially the variation of elemental concentrations on the sample. In this mode, the electron analyzer is set to accept electrons of a particular Auger peak. Since changes in signal amplitude can be caused by differences in elemental concentration, surface charging, or chemical bonding, there is much useful information available in Auger maps although care must be taken in their interpretation. For example, the low-energy Fe signal (~47 eV) is dependent on the chemical form of the iron.[10-12] For Fe oxides, this peak splits and the relative amplitude and position of the peaks are unique for each stoichiometric oxide.[12] Maps taken for slightly different electron energies can, therefore, be used to show the distribution of different chemical forms of Fe.

Table I. Samples and Treatments

Sample	Material	Treatment*
SD-A	Sputter-Deposited 304 SS	Vacuum anneal only
SD-1/4	Sputter-Deposited 304 SS	Oxidized 15 min
W-A	Wrought 304 SS	Vacuum anneal only
W-1/4	Wrought 304 SS	Oxidized 15 min
W-30	Wrought 304 SS	Oxidized 30 h
W-120	Wrought 304 SS	Oxidized 120 h

* All samples were vacuum annealed for 2 h at 1000 °C.

In addition to the Auger analysis, SEM/electron beam microprobe measurements were made on these samples. Although some new measurements are reported in this paper, most of the SEM work was included in Ref. 1.

RESULTS

The oxide layers on oxidized and annealed samples of both large- and small-grained material were quite different. The oxide formed on the samll-grained material was found to be uniform and rich in Cr. In contrast, the oxide on the large-grained material was nonuniform and rather patchy with an Fe oxide over grains and a Cr-rich oxide at grain boundaries. The surfaces of both coarse-grained and fine-grained annealed samples appeared visually uniform prior to air oxidation, but differences in composition were found. The small-grained annealed samples had more manganese on the surface and a greater oxygen concentration in the near-surface region than the large-grained annealed material. The final oxide morphology on the large-grained samples was sensitive to the sample treatment before oxidation, as indicated by a difference in the oxides formed on annealed and on annealed and repolished samples. The results are presented in detail below.

Oxidized Large-Grained Samples

The oxide formed on the large-grained material was not spatially uniform in composition or topography. An example of the surface formed is shown by an adsorbed-current micrograph of Sample W-1/4 (Fig. 1). The SEM and Auger data indicate that the larger unconnected areas cover grains, whereas the narrower connected areas are over grain boundaries.

Scanning Auger maps of Sample W-1/4 (Fig. 2) show an abundance of Cr at the grain boundary with a greater concentration of O over the grains. Maps taken for electron energy settings at 47 ev (Fe) and 50 eV (Fe oxide) show that the grain interiors have an Fe-oxide

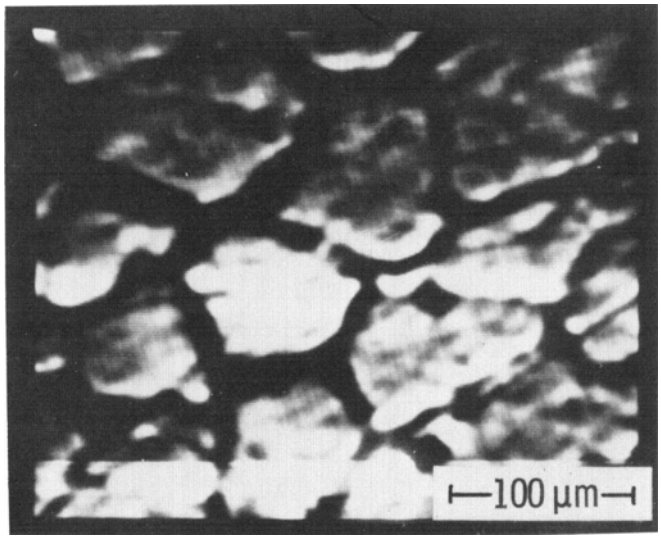

Fig. 1—Adsorbed-current image of Sample W-1/4.

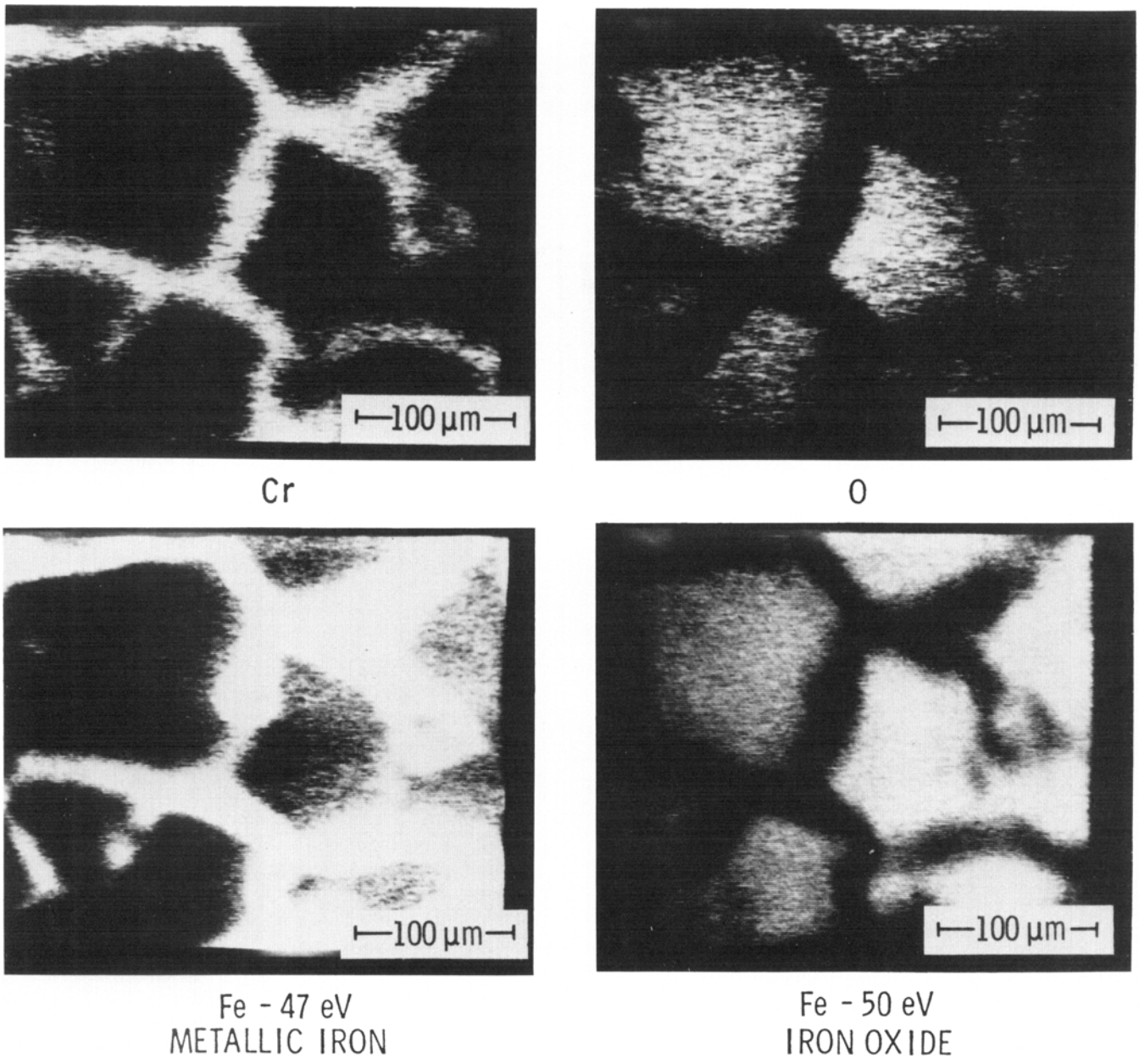

Fig. 2—Scanning Auger maps of Sample W-1/4 oberved during depth profile.

Auger signal. We also confirmed this result by Auger point scans in these areas as shown in Fig. 3, where the grain contains an Fe-oxide signal and the boundary a metallic Fe signal. The relative concentrations of the other elements can be observed by comparing the signal amplitudes. These scans confirm that the grain interior has little chromium and a great deal of O and oxidized Fe, whereas the grain boundary has more Cr, Ni and metallic Fe.

Sputter-depth profiles of grains and grain boundaries show that the relative composition of these two areas changes with depth. The sputter profiles for samples oxidized for 15 min and 30 h are shown in Figs. 4 and 5; although the depths of the oxidation are quite different, the shapes of the composition profiles are very similar. An oxide layer of fairly uniform composition formed over the grains, while a thin oxide of varying composition formed at the grain boundary. Iron oxide covers the grain interiors of each sample, and several hours of sputtering was not sufficient to remove the oxide from Sample W-30. Over the grain boundaries the concentrations of Fe, Ni, and Cr increased with depth and the oxygen slowly decreased for both samples. The approximate compositions at depths marked by arrows in the sputter profiles are listed in Table II.

The oxide formed over grains on W-1/4 was sufficiently thin to allow a sputter-depth profile through the oxide. Two observations made near the oxide-metal interface are of interest (Fig. 5): 1) the Fe concentration decreased and Cr and Ni increased before the interface; 2) Ni had a maximum concentration at the interface. The extent of these trends varied somewhat with location on the sample, but they are characteristic of the interface region.

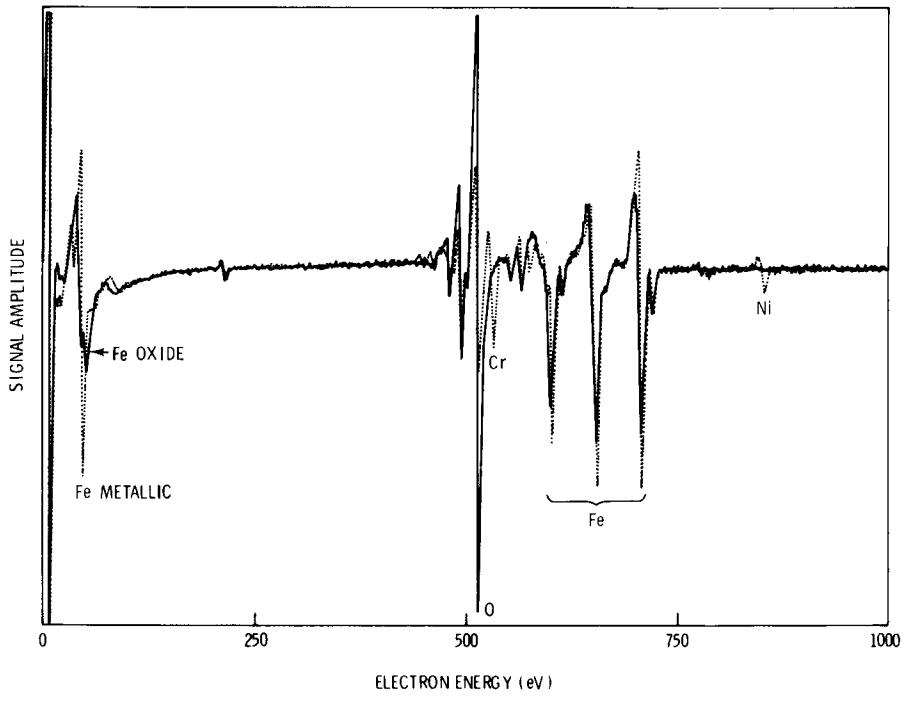

Fig. 3—Solid line is Auger signal amplitude as a function of energy for oxide over grain of Sample W-1/4. The dotted line is the Auger signal from a grain boundary region on the same sample.

Oxidized Small-Grained Samples

In contrast to the oxide formed on the large-grained material, the oxide on the small-grained, sputter-deposited material (SD-15) was uniformly distributed, both topographically to the eye and to the scanning Auger analysis. The compositional depth profile (Fig. 6) shows that a thin Cr-rich oxide, approximately 500Å thick, was formed on the sample. The compositional transition from the oxide to bulk material is rather gradual, and the depth of this transition is nearly identical to the depth of the oxide/metal transition region formed over the grain boundaries on the larger-grained sample oxidized for the same time (Fig. 5). The outer surface of the small-grained sample had a high concentration of Mn similar to that of the annealed small-grained sample (SD-A) and unlike that of all the large-grained, wrought samples. Because the Auger signals for Mn are partially obscured by the Fe Auger lines, it was not possible to observe Mn during the depth profile. However, our observations suggest that the Mn was mostly at the outer surface.

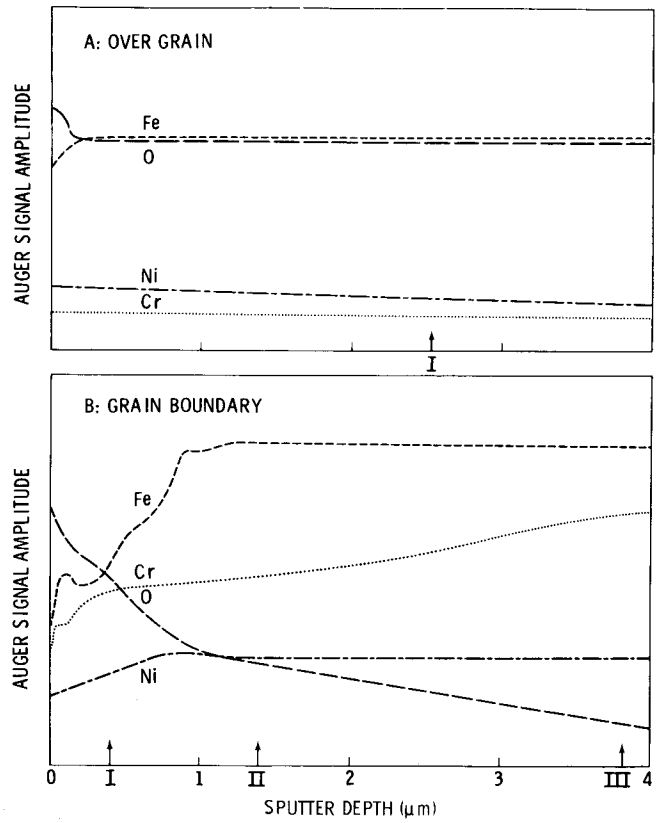

Fig. 4—Sputter-depth profiles of grain (*a*) and grain boundary (*b*) regions of sample W-30.

Annealed Samples (Not Oxidized in Air)

The surfaces of both the wrought and sputter-deposited samples were covered with a thin uniform oxide layer after the vacuum anneal at 1000 °C. This oxide was formed due to the presence of O in the quartz tubes during the anneal. There were, however, noticeable differences in the composition and sputter profiles of the two samples.

The small-grained sample (SD-A) had a 5 to 7 pct surface concentration of Mn, whereas the large-grained sample (W-A) had no observable Mn concentration. Thus, the surface concentration of Mn on the small-grained sample was four times greater than the bulk concentration of 1.5 pct Mn measured by Energy-Dispersive X-Ray Spectroscopy (EDX). The small-grained sample also had a greater near-surface concentration of oxygen compared to the large-grained material. This compositional difference was noted in the sputter-depth profiles of the two materials [Fig. 7]. The

Table II. Elemental Composition of Samples (At. Pct)

Sample	Treatment	Depth Indication*	Cr†	Fe	O	Ni	C	Comments
W-A	Wrought annealed	I	21	67	3	7	2	"Bulk" composition
SD-A	Sputter deposit annealed	I	21	63	6	6	3	"Bulk" composition
W-1/4	Wrought oxidized	AI	2	45	50	3	<2	Iron-rich oxide region
		AII	21	72	< 1	7.5	<2	"Bulk" composition
		BI	17	66	10	6	<1	Nearly to "bulk" composition
SD-1/4	Sputter oxidized	I	12	20	67	1	<2	Chromium-rich oxide
		II	20	64	7	6	<2	"Bulk composition"
W-30	Wrought oxidized	AI	< 2	41	56	3	<1	Iron-rich oxide region
		BI	9	30	56	3	2	Chromium oxide region
		BII	10	57	26	6	1	
		BIII	21	64	8	7	<6	"Bulk" composition

*As shown in Figs. 4 through 7.
†Chromium composition is less accurate in presense of large O signal.

oxygen displaced some Ni and Fe as indicated in the depth profile, suggesting that the oxygen was present as Cr oxide.

After most of the oxide layer was removed by sputtering, the elemental atomic compositions calculated for both materials were characteristic of 304 stainless steel. Because Auger signals from the various elements appear to have stopped changing with depth, these compositions are labeled "bulk" in Table II. However, it should be noted that 0.15 μm is a relatively small distance into the material and gradual changes in composition over greater distances will occur.

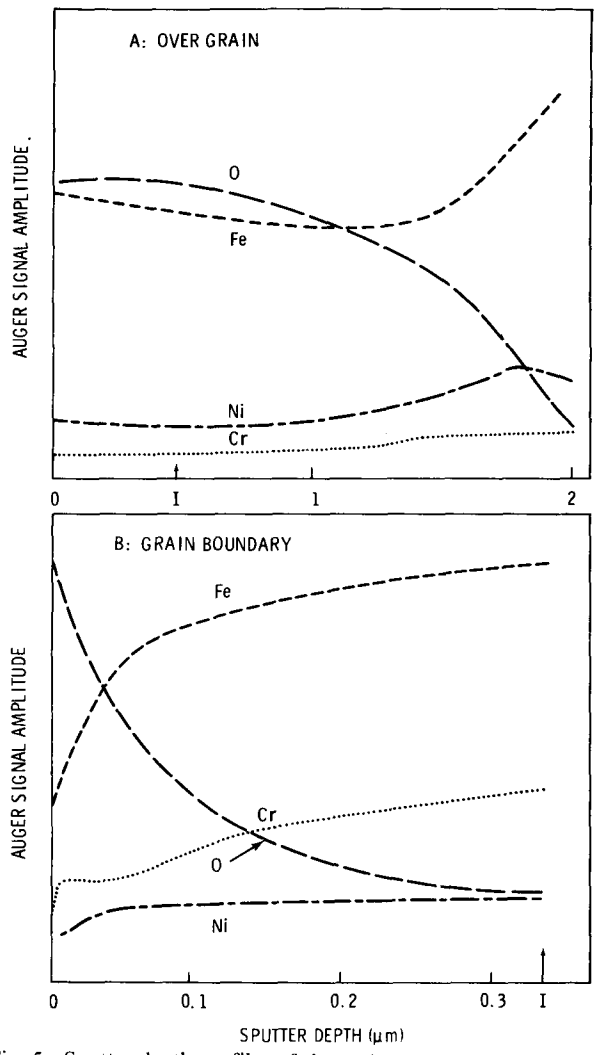

Fig. 5—Sputter-depth profiles of the grain (*a*) and grain boundary (*b*) regions of Sample W-1/4.

Oxidized Samples Polished Between Anneal and Oxidation

Sample pretreatment played a significant role in determining the morphology of the oxide on the large-grained material. SEM observations showed that the oxidation characteristics of a repolished, small-grained sample were the same as other small-grained samples; however, a repolished, larger-grained sample had a greater tendency to form a Cr-rich oxide than the nonrepolished large-grained samples.

DISCUSSION

The AES results show that a Cr oxide was preferentially formed near grain boundaries. One interpretation is that enhanced diffusion of Cr along grain boundaries allows small-grained material to form a protective oxide under conditions where large-grained material forms a duplex, nonprotective oxide structure.

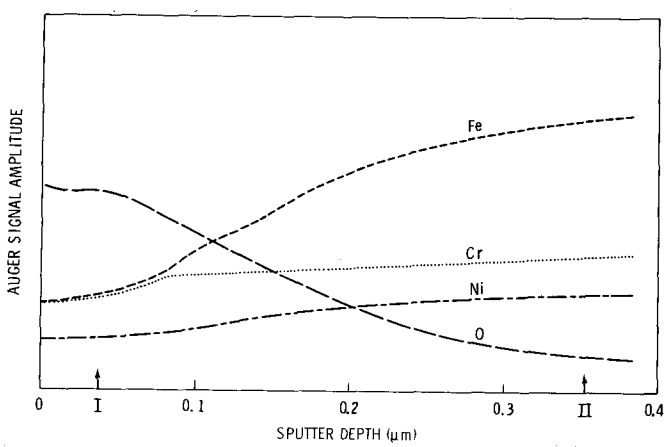

Fig. 6—Sputter-depth profile of oxidized small-grained (SD-1/4) sample.

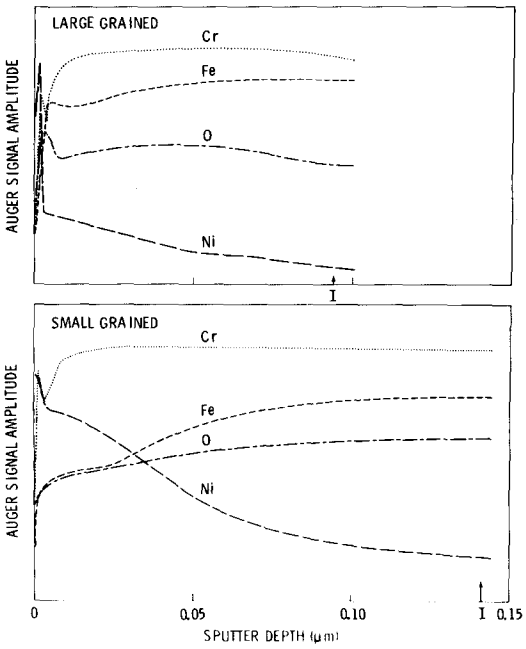

Fig. 7—Sputter-depth profiles of (*a*) annealed large-grained sample (W-A) and (*b*) annealed small-grained sample (SD-A).

Two mechanisms are suggested to explain the difference in oxide formation on annealed and repolished large-grained samples.

Oxidation—Large-Grained Material

The formation of two oxide phases on the large-grained material indicates a difference in elemental activity at grain boundaries and over grains. The grains are covered with a thick Fe-rich oxide of fairly constant composition as would be formed on Cr-poor materials.[6] The grain boundaries are protected with a relatively thin Cr-rich oxide similar in composition to that formed on the oxidized small-grained material. The presence of metallic Fe in the oxide over the grain boundary and Fe oxide over the grain interiors was indicated by the splitting of the low-energy iron MNN Auger peak for the oxide. The changes in this peak are well documented[10-12] and depend upon the composition of the oxide. Although the oxides formed over grain interiors are not necessarily stoichiometric, the shape of the MNN iron signal is similar to that of Fe_2O_3.[12] SEM analysis of the Fe-rich areas of oxidized samples also indicated the presence of Fe_2O_3. The material at the grain boundary was apparently Cr oxide with dissolved Fe which indicated the presence of sufficient Cr to reduce any Fe oxides formed during the oxidation. (These observations were not made at the outer surface where the low-energy Fe peak can be obscured by hydrocarbons, but after a few minutes of sputtering to remove surface contamination.)

The Fe-oxide/metal interface could be examined on Sample W-1/4 because the oxide formed over the grain interiors was thin enough to sputter through in reasonable time. The slight drop in Fe concentration and the increase in Cr and Ni near the interface indicated the presence of a second oxide phase. The split in the MNN Fe Auger signal began to disappear in this region, indicating a switch from oxide to metallic iron. SEM measurements show this region to be a $(FeCr)_2O_3$ spinel. The buildup of Ni at the metal-oxide interface has been observed before[8] and occurs because Ni is the alloy constituent that has the smallest energy of oxide formation.[13]

Oxidation—Small-Grained Samples

The oxide formed over the small-grained material was very similar to the oxide formed over the grain boundary of the larger-grained material. This effect was demonstrated both by similar trends in the depth profiles (compare Fig. 6 with Figs. 4(*a*) and 5(*a*)) and by comparable elemental compositions of the oxides. The flat region in the depth profile of the oxide on the small-grained material did not appear in the profile of the grain boundary region of the large-grained material [Figs. 5 and 6]. This may have been caused by a lateral spreading of the Cr oxide near grain boundaries for the large-grained samples, whereas an equilibrium condition has been established for the smaller-grained material. Because the depth profile of the Cr-rich oxide formed over the grain boundaries of the coarse-grained material does not have a region of constant composition, it is not possible to give "one" composition for this oxide. However, the composition of the oxide over the small-grained material (SD-1/4) was similar to that found at position BI during the profile of the large-grained Sample W-30.

Relationship to Oxidation of Nickel-Chromium Alloys

The basic features of the oxidation of 304 stainless steel found in this study are also observed in NiCr alloys. The selective formation of Cr_2O_3 at grain boundaries has been well established for NiCr alloys[3-5] and is related either to enhanced Cr diffusion along grain boundaries or to nucleation of Cr_2O_3 in the grain boundaries. For NiCr alloys with less than 20 pct Cr, Cr_2O_3 is formed at grain boundaries during the initial stages of oxidation while NiO, $NiCr_2O_4$ and Cr_2O_3 are formed away from the grain boundary. At very low oxygen partial pressure, the only external oxide formed is Cr_2O_3 at the grain boundary. Chromium diffuses laterally from the grain boundary over the alloy, increasing the spread of external Cr_2O_3. This mechanism of oxidation causes small-grained material to form a protective Cr_2O_3 layer more quickly than large-grained material. In fact, the layer may never be established on the large-grained sample if the oxidation rates do not allow the volume fraction of Cr_2O_3 to reach the value required for the formation of a continuous Cr_2O_3 layer. For 304 stainless steel, therefore, the tendency of Cr_2O_3 to form at grain boundaries and spread laterally can explain many of the differences observed in the oxidation of large- and small-grained material as reported here.

Vacuum Annealing

The major differences found in the large- and small-grained samples after the vacuum anneal may also influence oxide formation. Analysis of samples after vacuum anneal and before oxidation in air showed large differences in the O and Mn content in the surface region of large- and fine-grained material. A region of somewhat constant O composition appeared in the depth profile of the small-grained material [Fig. 7] and suggested that an oxide had started to form in the surface region of the sample. Oxygen content of this small-grained, annealed sample at 0.25 μm depth was roughly 26 at. pct. The fine-grained, sputter-deposited material had more O in the surface region than the wrought samples; the reason for this effect is not clear. Small amounts of O may have been introduced as an impurity during the sputter process, but the depth profiles indicate that at a depth of 1 μ or greater neither large or fine-grained samples had excess oxygen. It seems more likely that oxidation during the vacuum-anneal pretreatment was different for the two types of samples, possibly because of O penetration along the grain boundaries.

The primary purpose of the vacuum anneal was to stabilize grain size for both materials (in addition to effecting a bcc to fcc phase transformation for the sputter-deposited material). The anneal also decreased the density of crystal defects. Evaporation of Mn, Cr and Fe from such Fe-Cr-Ni alloys is known to occur during a 1000 °C vacuum anneal[14-15] and would alter the composition and oxidation properties of the outer surface of the samples. For example, Wild[14] observed a 25 pct decrease in the Cr surface concentration for 18Cr-9Ni stainless steel after just 15 min of vacuum anneal at 1000 °C. However, no Cr depletion occurred in our annealed samples because of the small volume of the quartz tubes in which the samples were heated. The equilibrium Cr vapor pressure for 1000 °C was easily reached with very little material transported away from the sample. The absence of any major Cr depletion was apparent in the sputter-depth profiles of the annealed samples. There was a reaction between O present in the quartz tube with the Cr and Mn in the sample to form the thin oxide observed after the pretreatment.

Effects of Pretreatment on Oxidation—Repolished Samples

The single phase oxide formed on the annealed and repolished large-grained sample when contrasted with the duplex oxide formed on the annealed samples showed that the ability of Cr_2O_3 to nucleate and form a protective oxide was altered by the polishing treatment. Earlier Auger studies by Stoddard and Hondros[7] and Betz *et al*[8] on wrought stainless found Cr_2O_3 to be the primary oxide formed. The major difference between the current samples and those of the earlier studies was the vacuum anneal pretreatment. On the other hand, annealing and repolishing had little effect on the oxidation behavior of the small-grained material. Consequently, we conclude that the excess O observed in the surface region of the annealed, small-grained sample had little effect on later oxidation in air.

Two mechanisms could account for the differences in the oxides formed on annealed and on annealed and repolished large-grained samples. First, it is well known that cold-worked, polished, and other high-defect materials have different corrosion properties than those of nondamaged material.[16] The enhanced diffusion of Cr in defect regions allows the formation of a Cr-rich oxide.[3] Thus, repolishing may have increased Cr diffusivity in the surface region and thereby allowed the formation of a Cr-rich oxide on the large-grained samples. This process would also occur on other samples that had been cold-worked before oxidation. Second, it is also known that oxidation occurs selectively at grain boundaries during low-pressure oxidation of NiCr alloys.[5] We suggest that a thin oxide formed at grain boundaries during our pretreatment could inhibit the diffusion of Cr during later oxidation in air. Both small- and large-grained materials would be affected by this process, but the lateral spreading of external Cr_2O_3 from grain boundaries may be fast enough to allow formation of a protective layer only for the small-grained samples. A narrow oxide formed at the grain boundary could not be observed directly by our 2.5 μm electron beam. However, O penetration into many grain boundaries of the fine-grained material could produce an O profile similar to what we observe in Fig. 7 for the fine-grained annealed sample.

Regardless of the mechanism, it is clear that pretreatment significantly altered the morphology of the oxide formed on the large-grained material in air. Since spalling of an oxide is often affected by nonuniformity,[17-20] pretreatments that enhance a difference in oxides formed over grains and at grain boundaries are particularly important.

Manganese Oxide

The Mn observed on oxidized and annealed small-grained samples is probably in the form of MnO, which is the most stable binary oxide likely to form on this alloy.[13] An enhanced diffusivity of Mn in the samples due to the large number of grain boundaries may account for the relatively large amount of Mn at the surface. A large amount of Mn was also observed by SEM in oxides formed on fine-grained material oxidized for long times.[1] The Auger results show that the Mn-rich outer layer forms very quickly on the fine-grained material, but not on large-grained material. The role of Mn in the formation of the protective oxide is not clear, particularly since Mn is normally a detrimental addition to stainless steel from the view of oxidation resistance.[2]

SUMMARY

This AES study of oxidized large and small-grained stainless steel supports the view that Cr_2O_3 selectively forms at grain boundaries and spreads along the surface. Therefore, small-grained material (either uniformly small-grained or material with a recrystallized surface) will form a protective Cr_2O_3 oxide more easily than large-grained material. The influence of annealing

and polishing on the oxide formed on the large-grained material indicates that the availability of Cr to the surface of this material is at a critical level, such that relatively small changes in the material can appreciably alter the stages of oxide formation.

CONCLUSIONS

Thick Fe oxides of relatively constant composition were formed over grains of vacuum-annealed, large-grained (40 μm) 304 stainless steel samples oxidized in air at 800 °C. On the other hand, thin, Cr-rich oxides are formed at the grain boundaries.

The oxide formed on vacuum-annealed, small-grained material ($\sim$4 μm) at 800 °C was uniform over the sample, relatively thin, and Cr-rich. Auger electron spectroscopy analysis indicated that the depth profile of this oxide was similar to that of the oxide formed over the grain boundaries of the large-grained material.

A thin oxide formed on both large-grained and small-grained samples during the vacuum-anneal pretreatment. Removing this oxide by polishing did not alter the air oxidation behavior of the small-grained samples, but did promote the formation of a Cr-rich oxide on the large-grained material. The difference in oxide formation on polished and nonpolished, large-grained samples was attributed to removal of pre-oxidized regions by polishing and to differences in oxidation behavior caused by polishing-induced surface deformations.

Auger electron spectroscopy enabled the detection of a thin surface layer of MnO in small-grained material after pretreatment and after oxidation in air. High mobility of Mn in grain boundaries presumably allows enough Mn to reach the surface to form the very stable oxide layer.

The overall oxidation behavior of both small- and large-grained material was consistent with selective formation of Cr_2O_3 at grain boundaries followed by lateral diffusion of Cr and spreading of Cr_2O_3. This mechanism accounts for the formation of continuous Cr_2O_3 films on small-grained material under conditions where a similar film may not form on larger-grained materials.

ACKNOWLEDGMENTS

The authors gratefully acknowledge several helpful discussions with D. P. Whittle, J. T. Prater and M. T. Thomas concerning interpretation of the results. This work was supported by the Division of Materials Sciences, Office of Basic Energy Sciences, U.S. Department of Energy under contract DE-AC06-76RLO-1830.

REFERENCES

1. M. D. Merz: *Met. Trans. A.*, 1979, vol. 10A, p. 71.
2. A. J. Sedriks: *Corrosion of Stainless Steels*, p. 242, John Wiley and Sons, New York, NY, 1979.
3. B. Chattopadhyay and G. C. Wood: *J. Electrochem. Soc*, 1970, vol. 117, p. 1163.
4. C. S. Giggins and F. S. Pettit: *Trans. TMS-AIME*, 1969, vol. 245, p. 2495.
5. C. S. Giggins and F. S. Pettit: *Trans. TMS-AIME*, 1969, vol. 245, p. 2509.
6. J. C. Kolleen, A. E. Smith, and R. K. Wild: *Corros. Sci.*, 1976, vol. 16, p. 551.
7. C. T. H. Stoddart and E. D. Hondros: *Nat. Phys. Sci.*, 1972, vol. 237, p. 90.
8. G. Betz, G. J. Wehner, and L. Toth: *J. Appl. Phys.*, 1974, vol. 45, p. 5312.
9. L. E. Davis, N. C. MacDonald, P. W. Palmberg, G. E. Riach, and R. E. Weber: *Handbook of Auger Electron Spectroscopy*, Physical Electronics Industries, Eden Prairie, 1976.
10. G. Ertl and K. Wandett: *Surf. Sci.*, 1975, vol. 50, p. 479.
11. G. C. Allen and R. K. Wild: *J. Electron. Spectros. Relat. Phenom.*, 1974, vol. 5, p. 409.
12. M. Seo, J. B. Lumsden, and R. W. Staehle: *Surf. Sci.*, 1975, vol. 50, p. 541.
13. T. B. Reed: *Free Energy of Formation of Binary Compounds*, MIT, Cambridge, MA, 1971.
14. R. K. Wild: *Corros. Sci.*, 1974, vol. 14, p. 575.
15. L. J. Weirick: SCL-DC-7220091, Sandia Laboratories, Livermore, CA, 1973.
16. M. Warzee, J. Hennaut, M. Maurice, C. Sonnen, and J. Waty: *J. Electrochem. Soc.*, 1975, vol. 112, p. 670.
17. V. R. Howes: *Corros. Sci*, 1970, vol. 10, p. 99.
18. J. Webber: *Corros. Sci.*, 1976, vol. 16, p. 499.
19 R. K. Wild: *Corros. Sci.*, 1977, vol. 17, p. 87.
20. V. R. Howes: *Corros. Sci.*, 1968, vol. 8, p. 729.